
Characterisation of charge transport in compound semiconductor detectors

P.J. Sellin, H El-Abbassi, A.Galbiati, S.Rath

Radiation Imaging Group

Department of Physics

University of Surrey

Guildford, UK

p.sellin@surrey.ac.uk

Issues for new detector materials

❑ Material uniformity

- monocrystalline vs polycrystalline
- mechanical defects, eg. pipes and twins
- distribution of electrical traps

❑ Metal - Semiconductor contacts

- contact technologies
- ohmic vs blocking contacts
- Electric field profile and I-V characteristics

❑ Charge Transport

- $\mu\tau$ products for electrons and holes \Rightarrow CCE
- MIPS S/N ratio

❑ Radiation Hardness

- effect on trap concentrations, IV, CCE

Contact-less mapping techniques:
photoluminescence,
cathodoluminescence, resistivity

Nuclear microbeam (IBIC)
imaging

I-V, barrier heights

Field mapping: IR, Franz-
Keldysh imaging

Radioisotopes

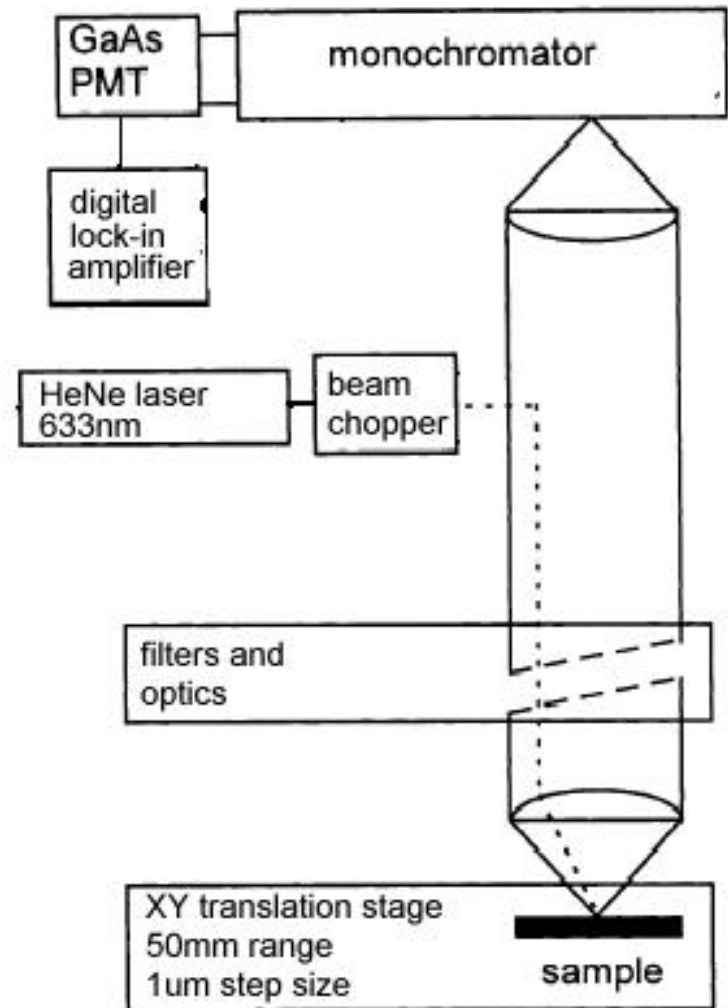
Irradiation measurements

Transient spectroscopy -
PICTS, DLTS

Whole wafer photoluminescence mapping

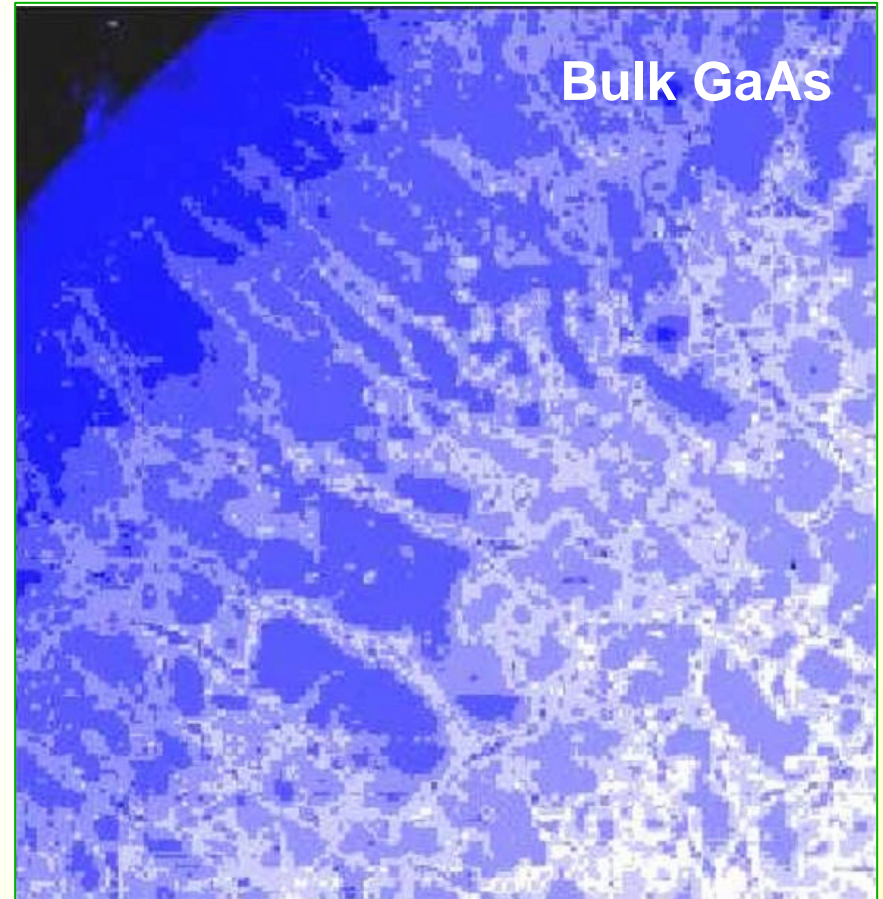
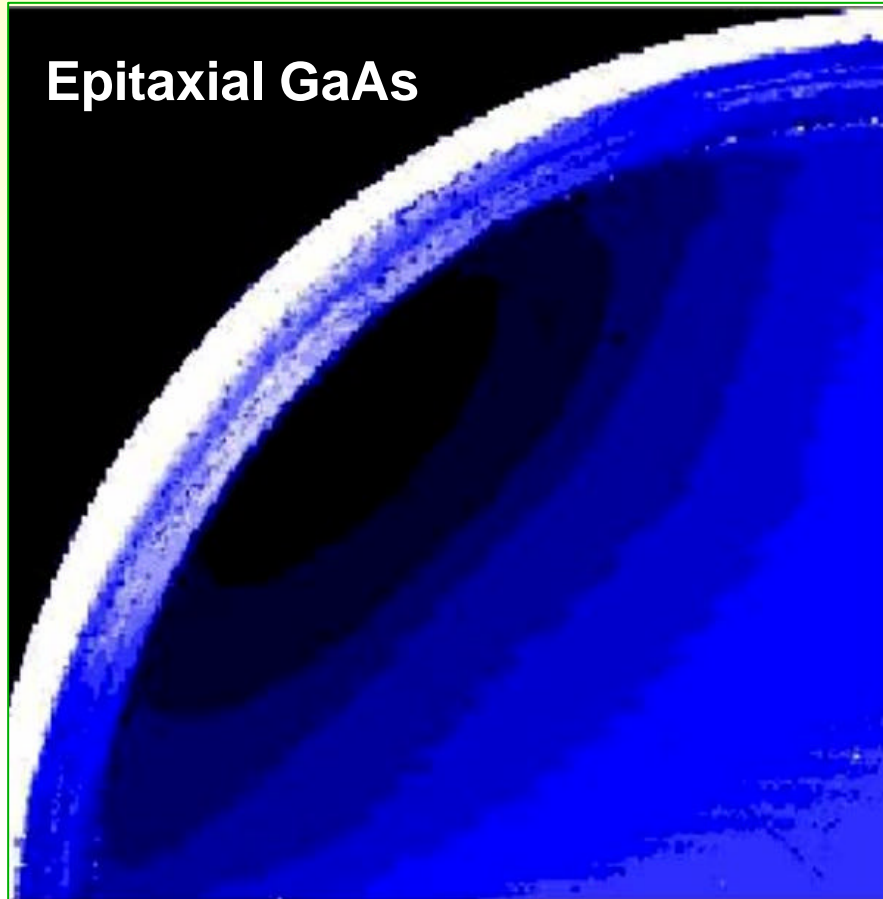
Material uniformity can be characterised using room temperature photo-luminescence mapping - a contact-less, whole wafer technique:

- ❑ A 25 mW 633 nm HeNe laser is focussed to $\sim 50 \mu\text{m}$ on the wafer
- ❑ the wafer is mounted on an XY stage, and scanned
- ❑ PL intensity maps at peak the band edge emission wavelength (eg. 870nm for GaAs) are acquired

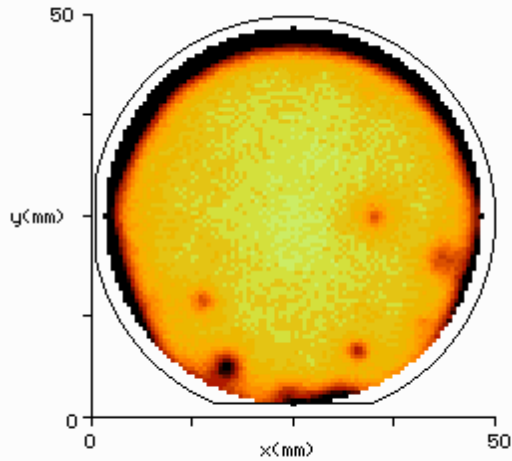


PL maps of GaAs

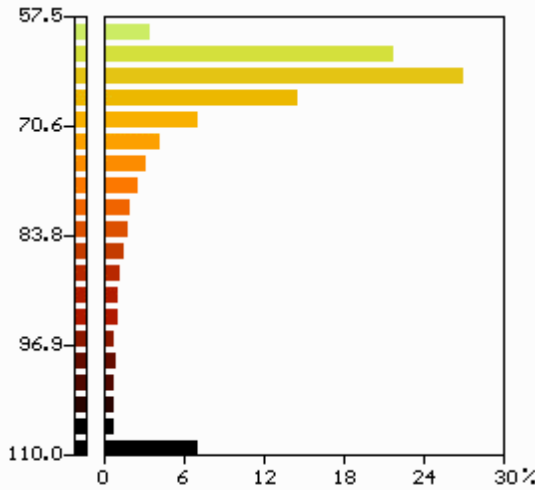
Photoluminescence mapping clearly shows the uniformity of epitaxial GaAs compared to semi-insulating VGF material:



Resistivity mapping of GaAs wafers

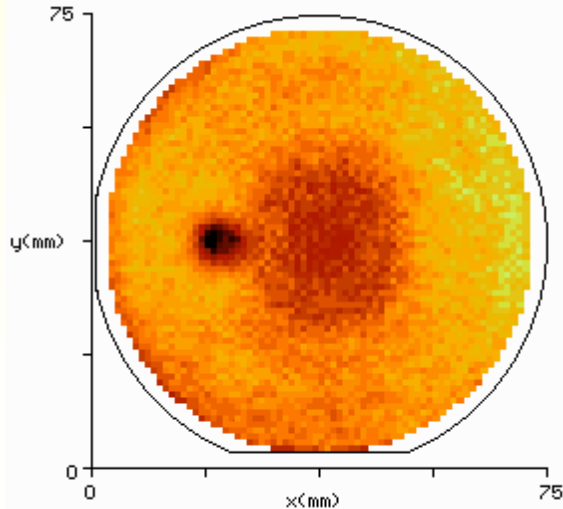


Acrotec D/4111AUN/W189

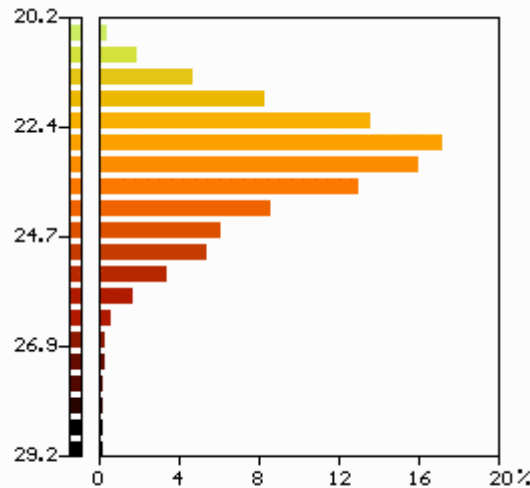


Contact-less resistivity mapping using the Time Dependent Charge Method has been pioneered at Freiburg

The wafer forms a capacitor dielectric where the time dependence of the discharge depends on the resistivity



Freiburger 45120-W04



R. Stibal et al, Semicond. Sci. Technol. 6 (1991) 995-1001

Mu-tau products in new materials

Compound semiconductors often exhibit low mobilities - particularly holes - and short carrier lifetimes.

In order to maximise the induced signal (CCE), both the field strength E and the mu-tau product $\mu\tau$ must be maximised:

$$CCE = \frac{Q}{Q_0} = \frac{I}{d} \quad I = mtE$$

Semi-insulating materials are often compensated by doping.

Requirements for new materials are typically:

- **high purity material**, to minimise residual impurity concentration
- **minimal** doping to avoid over compensation and maximise lifetimes
- well-controlled doping, **uniform** over the wafer surface

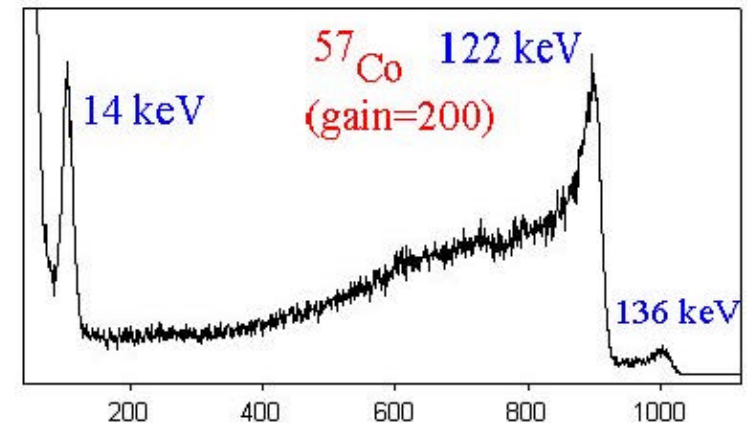
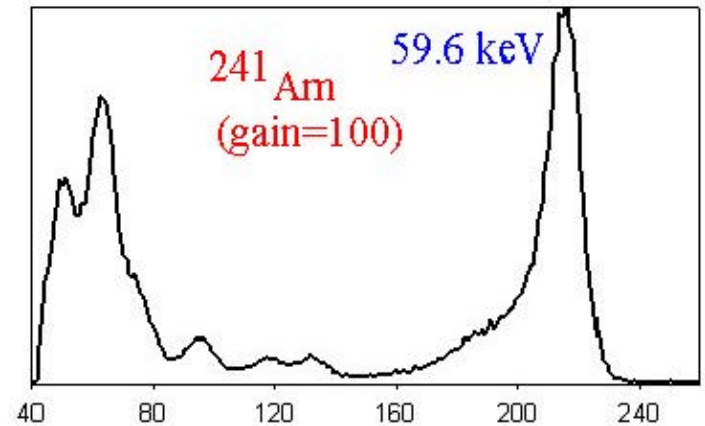
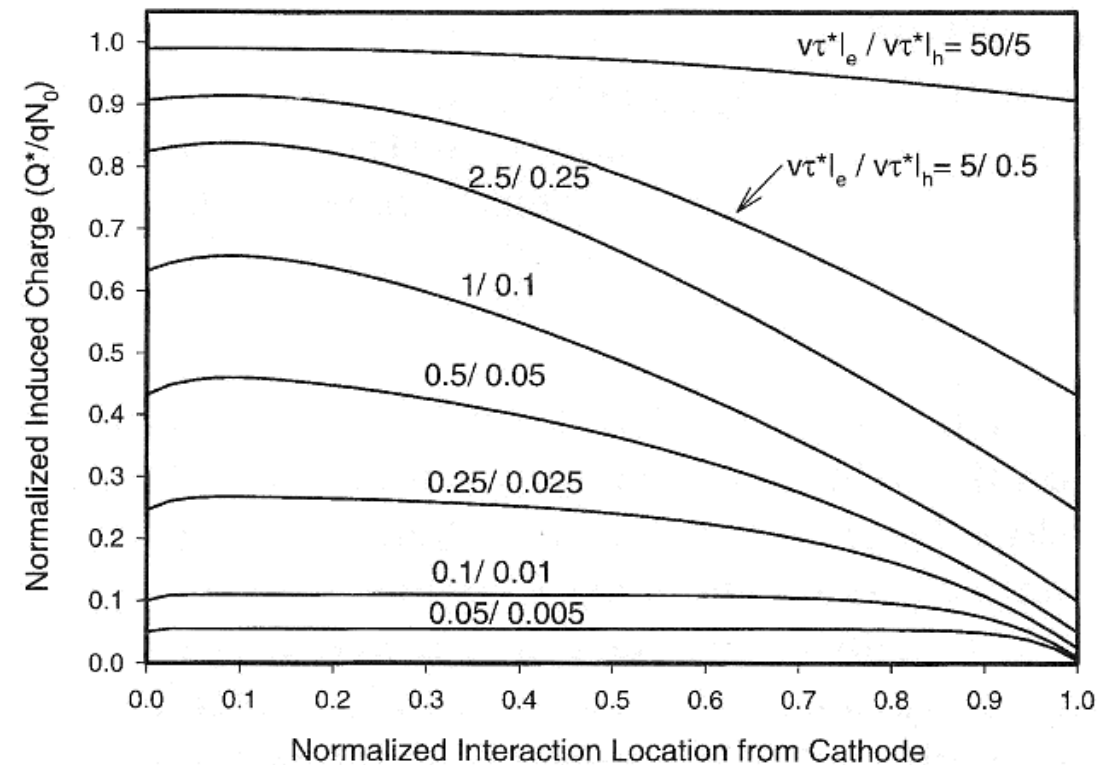
Radioisotope spectroscopy routinely gives CCE - *spatially resolved methods give CCE imaging*

⇒ Correlation with CCE imaging and material uniformity/properties

Poor hole transport affects gamma ray spectroscopy

Low hole $\mu\tau$ values cause depth-dependent charge collection efficiency

⇒ 'hole tailing' in CdZnTe shows characteristic asymmetric gamma ray peaks



For MIPs, severely reduced hole transport causes:

⇒ reduced S/N ratio

⇒ depth-dependent signals could degrade position resolution

Paul Sellin, Radiation Imaging Group

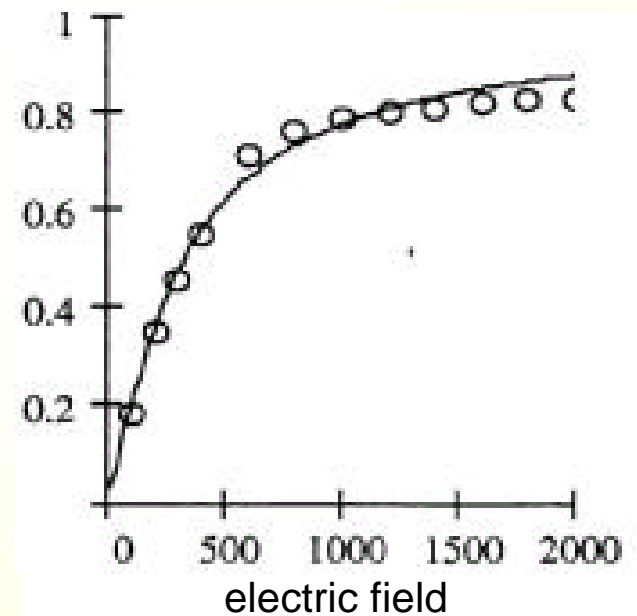
Mobility-Lifetime products

Mobility-lifetime products are normally measured from alpha particle spectra - cathode (*anode*) irradiation is sensitive to electron (*hole*) transport.

$$\text{Generally: } \text{CCE} = \frac{Q}{Q_0} = (\mu_e t_e + \mu_h t_h) E$$

The Hecht equation is used, eg. for cathode irradiation with alphas:

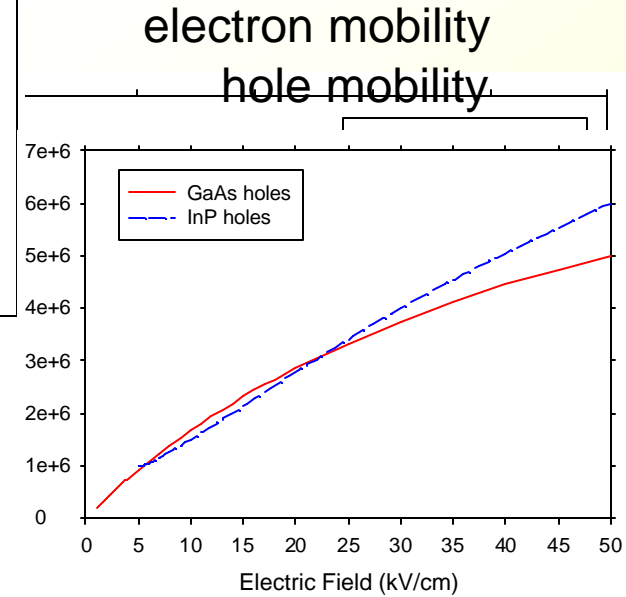
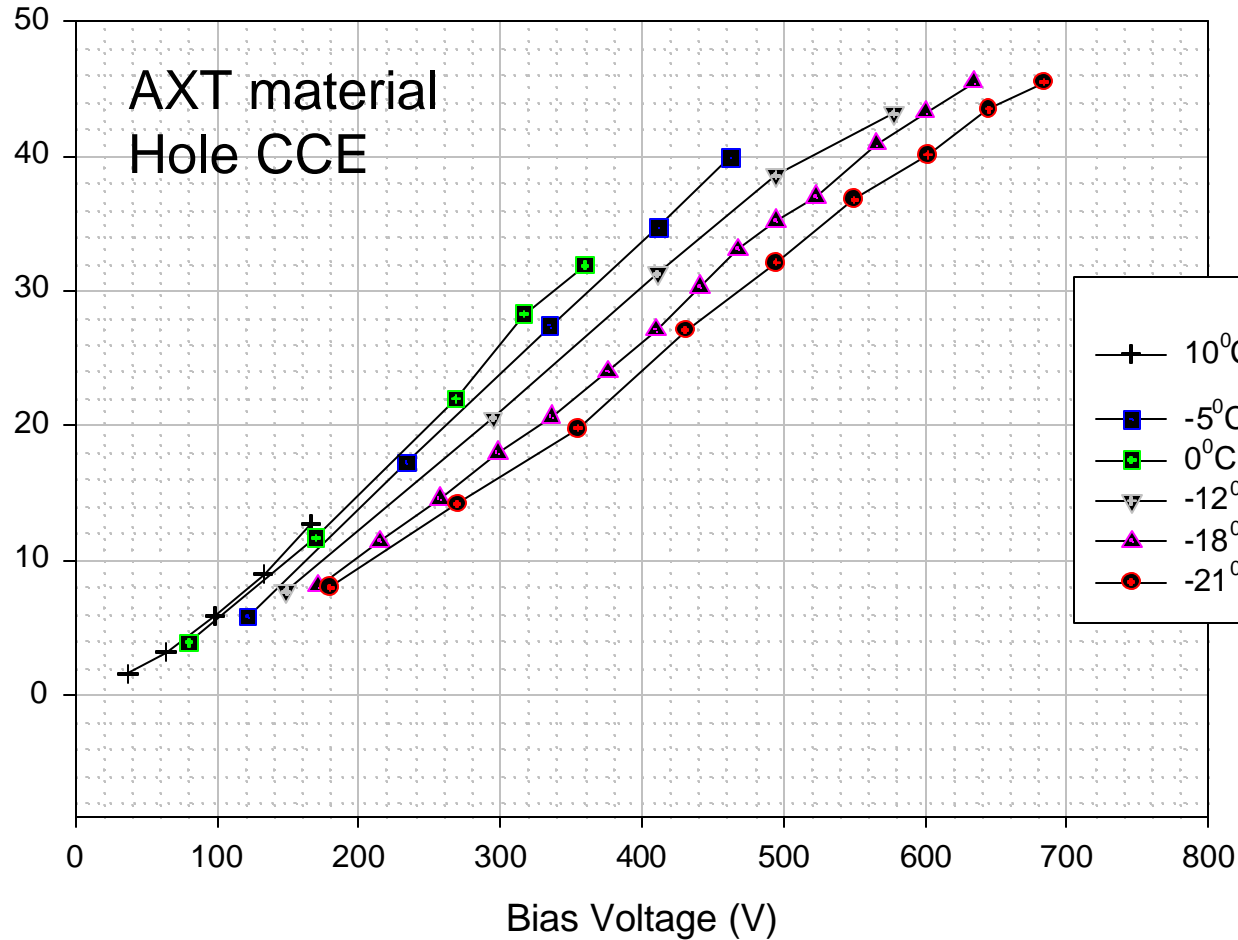
$$\text{CCE} = \frac{Q}{Q_0} = \frac{\mu_e t_e V}{d^2} \left[1 - \exp\left(-\frac{1 - \frac{x}{d}}{\frac{\mu_e t_e V}{d^2}}\right) \right]$$



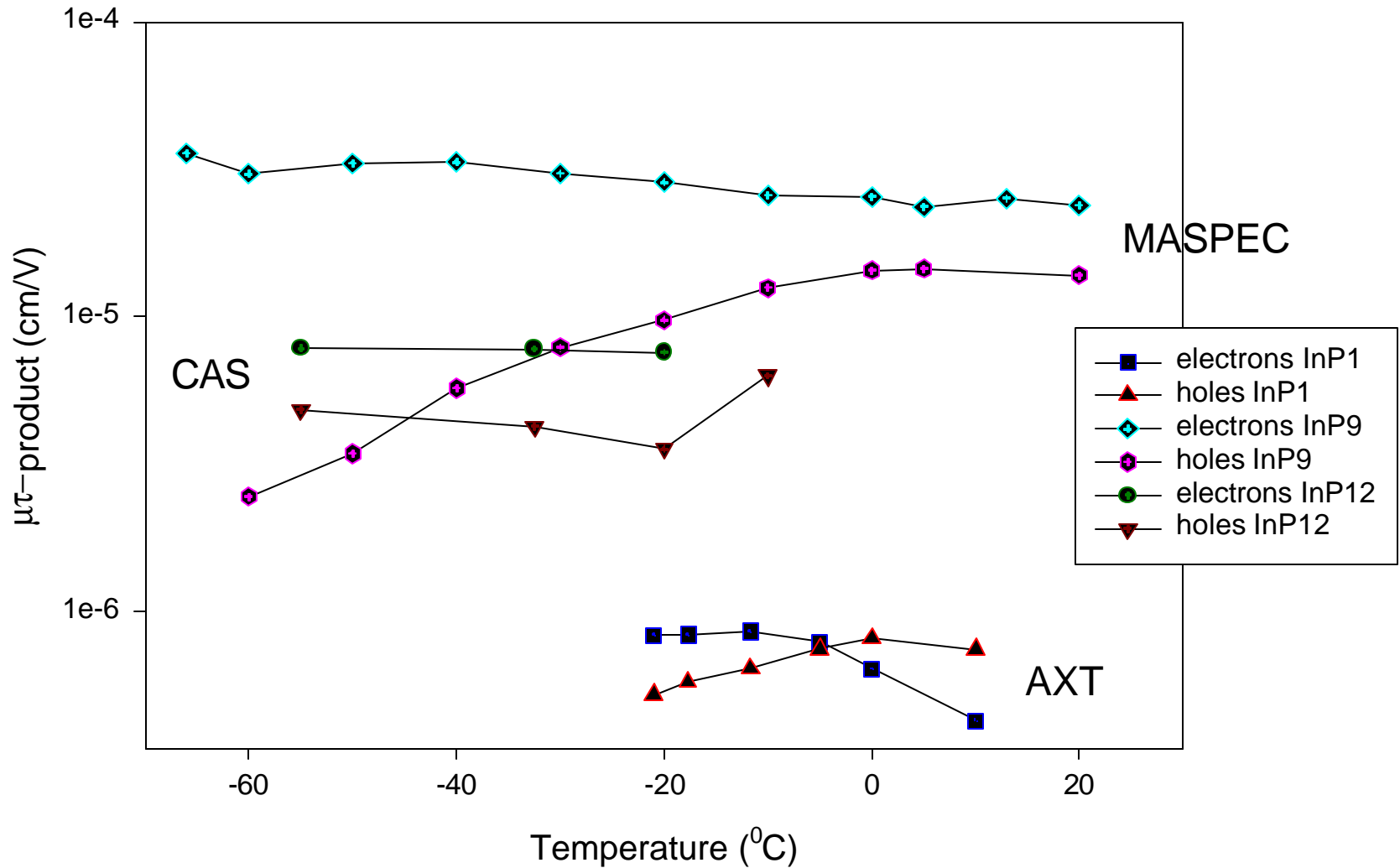
Hence fitting relative peak position as a function of electric field extracts $\mu_{e(h)} t_{e(h)}$ for cathode and anode irradiation respectively

Alpha particle CCE in InP detectors

Temperature dependent CCE was measured for electrons and holes in InP detectors



InP mu-tau product vs Temperature



Different InP samples show variations in $\mu\tau$ values over a 50x range - reflecting the material purity and Fe doping concentration

Polycrystalline Materials

Some promising materials are truly polycrystalline, and have the potential for large area sensors:

- ❑ CVD diamond, supplied as free-standing films with thickness of typically 50 - 300 μm
- ❑ Polycrystalline amorphous silicon, CdTe and HgI_2

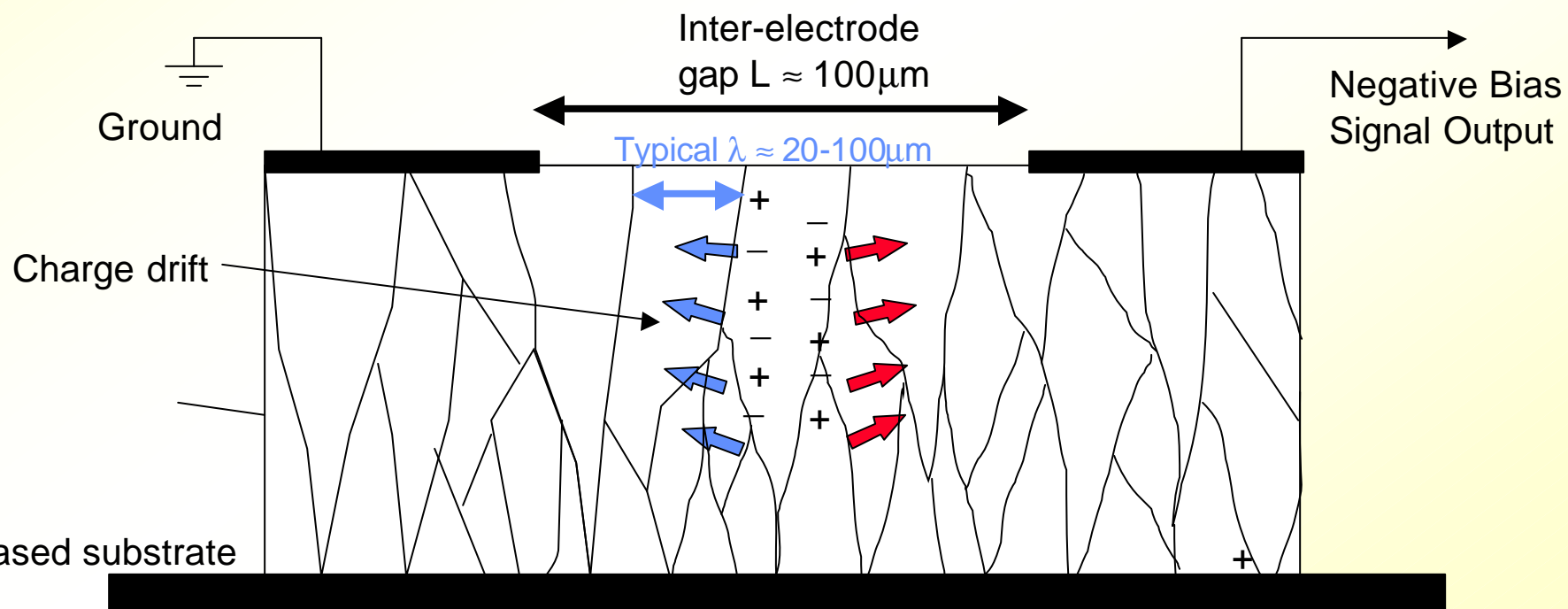
CVD diamond has been studied extensively by the HEP community:

- excellent radiation hardness
- minimal leakage currents, low noise
- robust technologies for contacts and bonding
- charge signal per MIP is low
- charge trapping can cause CCE <100%
- cost for large area detectors

Ion Beam imaging of polycrystalline materials

Charge transport uniformity is particularly important for polycrystalline materials, eg. a-Si and CVD diamond

Ion Beam imaging provides micron resolution imaging of CCE, allowing correlation of detector performance to material properties



The Surrey Ion Beam Microprobe



3 MeV protons or 6 MeV alpha particles, with event rates on the sample of 100 Hz - 1 kHz

Paul Sellin, Radiation Imaging Group

Scanning of CCE vs depth using lateral ion-beam induced charge microscopy

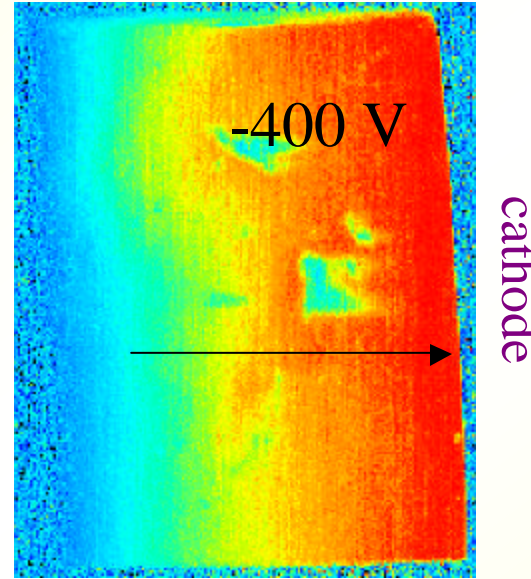
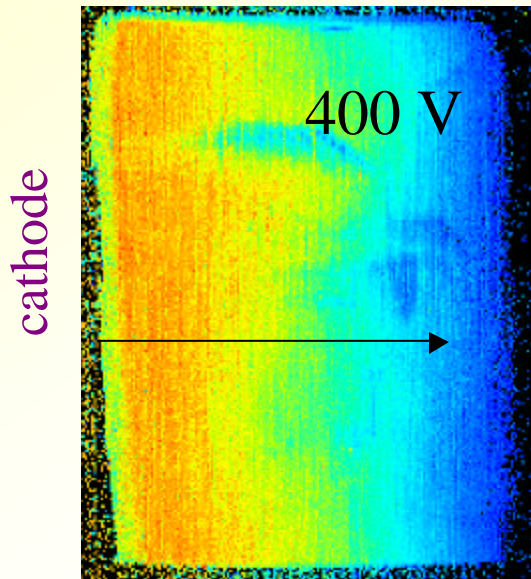
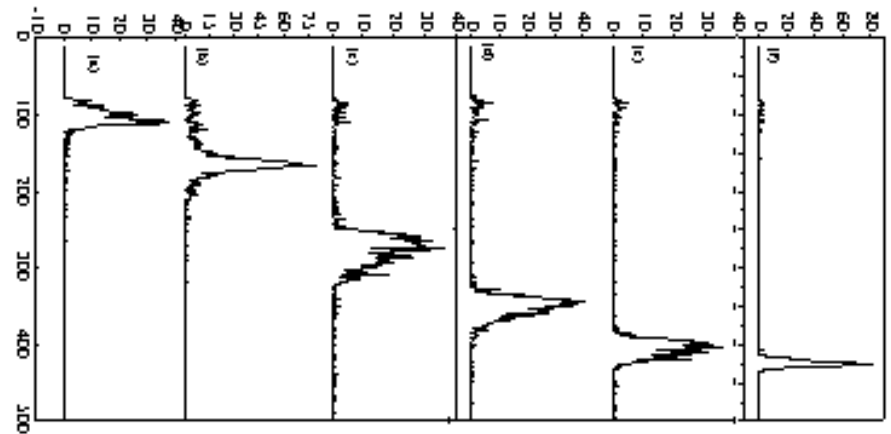
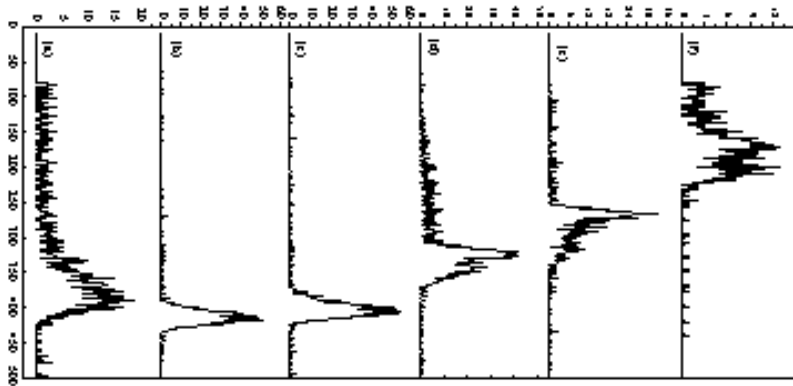


Image of CCE using $1\mu\text{m}$ resolution 2MeV scanning proton beam



+400 V

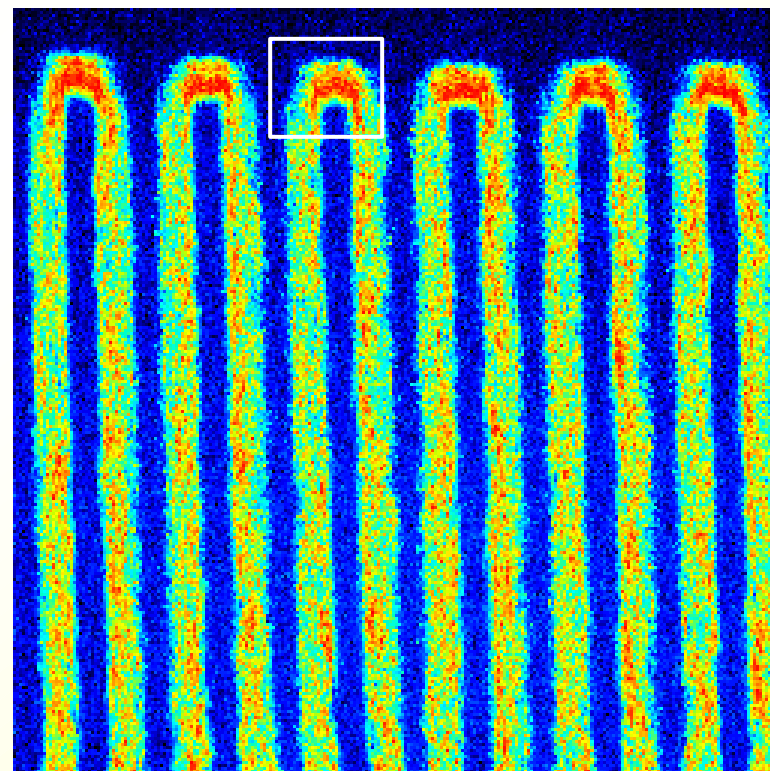
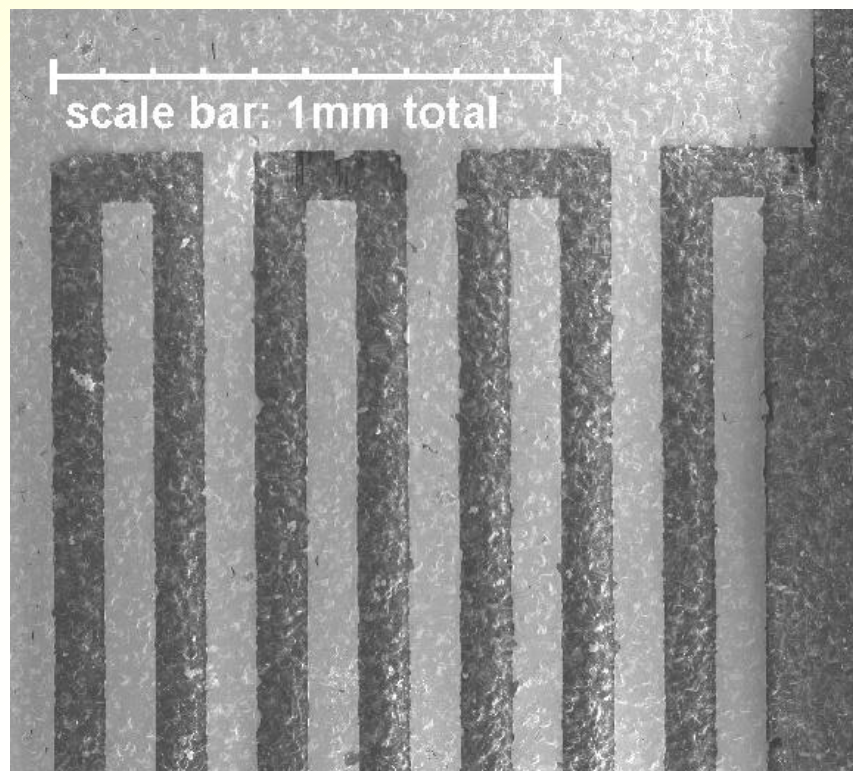
-400 V

Pulse height spectra as a function of depth

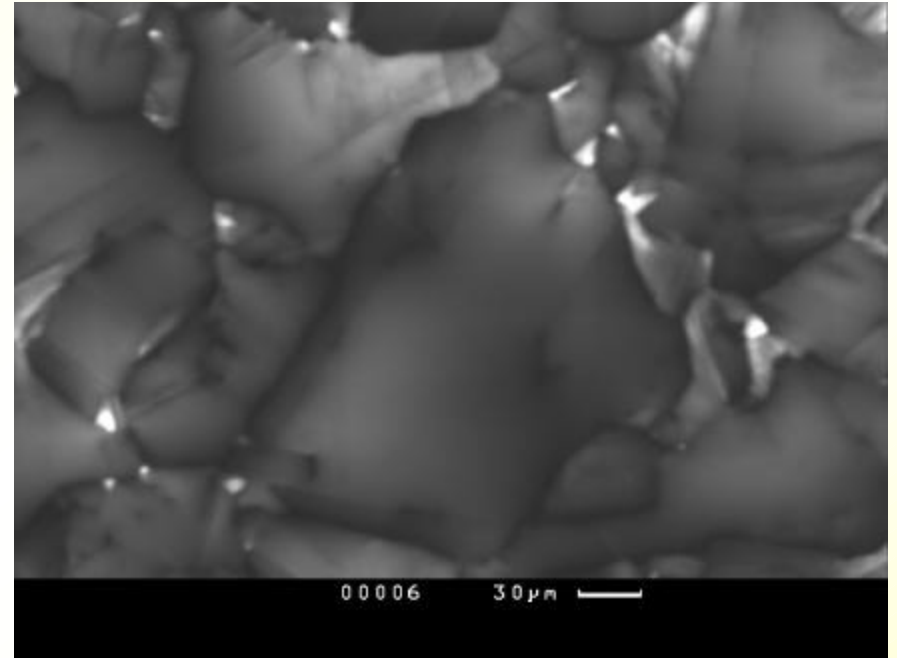
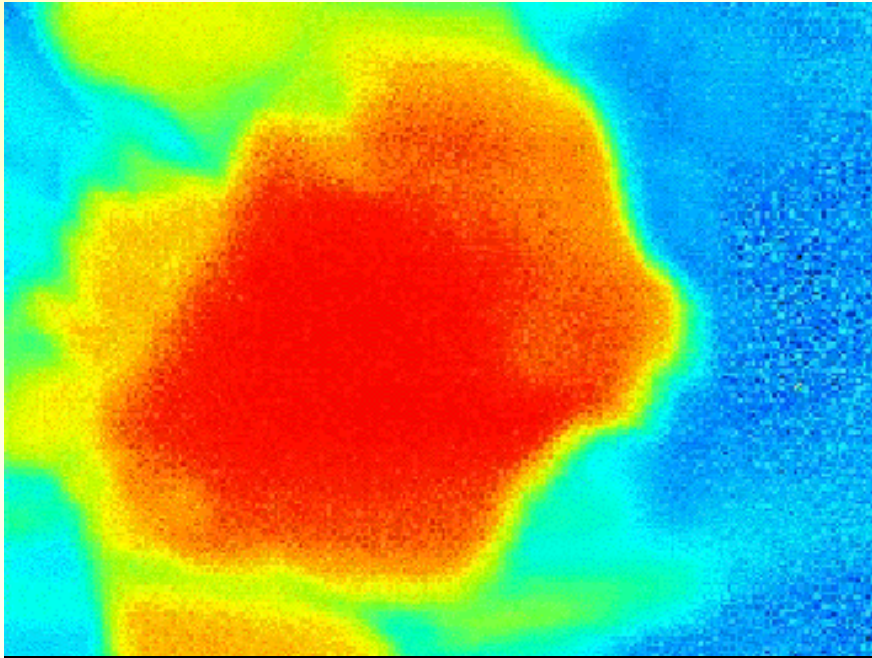
IBIC imaging of diamond with 2 MeV protons

The Surrey University microprobe performs Ion Beam Induced Charge (IBIC) imaging with a 1 micron resolution 6 MeV proton beam

IBIC maps show 'hot spots' at electrode tips due to concentration of the electric field



Single crystallite imaging

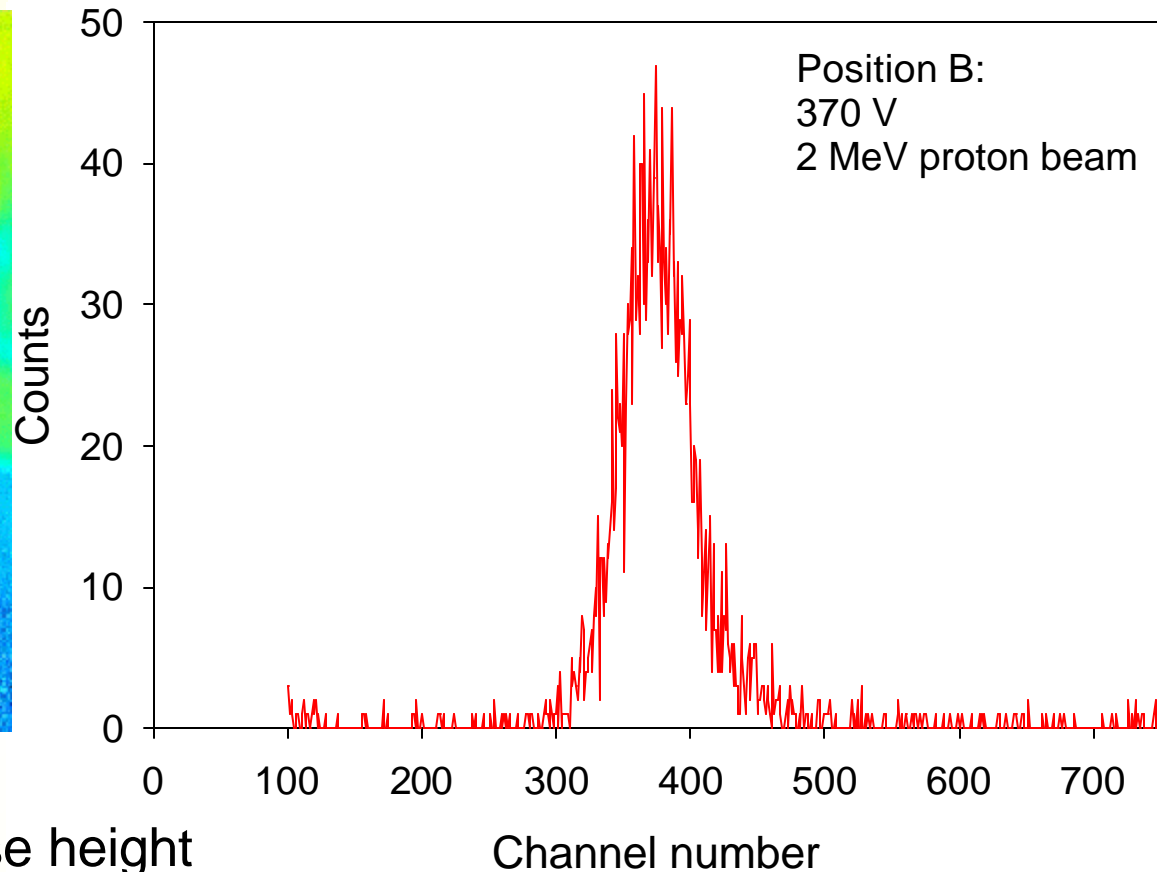
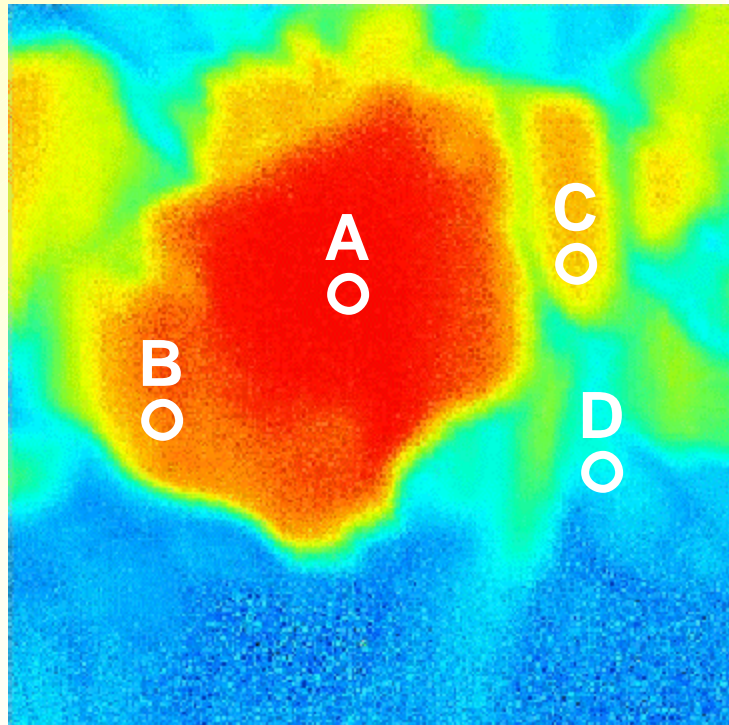


Simultaneous SEM and CL images show the morphology of a small region of a diamond strip detector

The large crystallite is $\sim 120\mu\text{m}$ wide by $\sim 150\mu\text{m}$ high, and is positioned centrally between two electrodes.

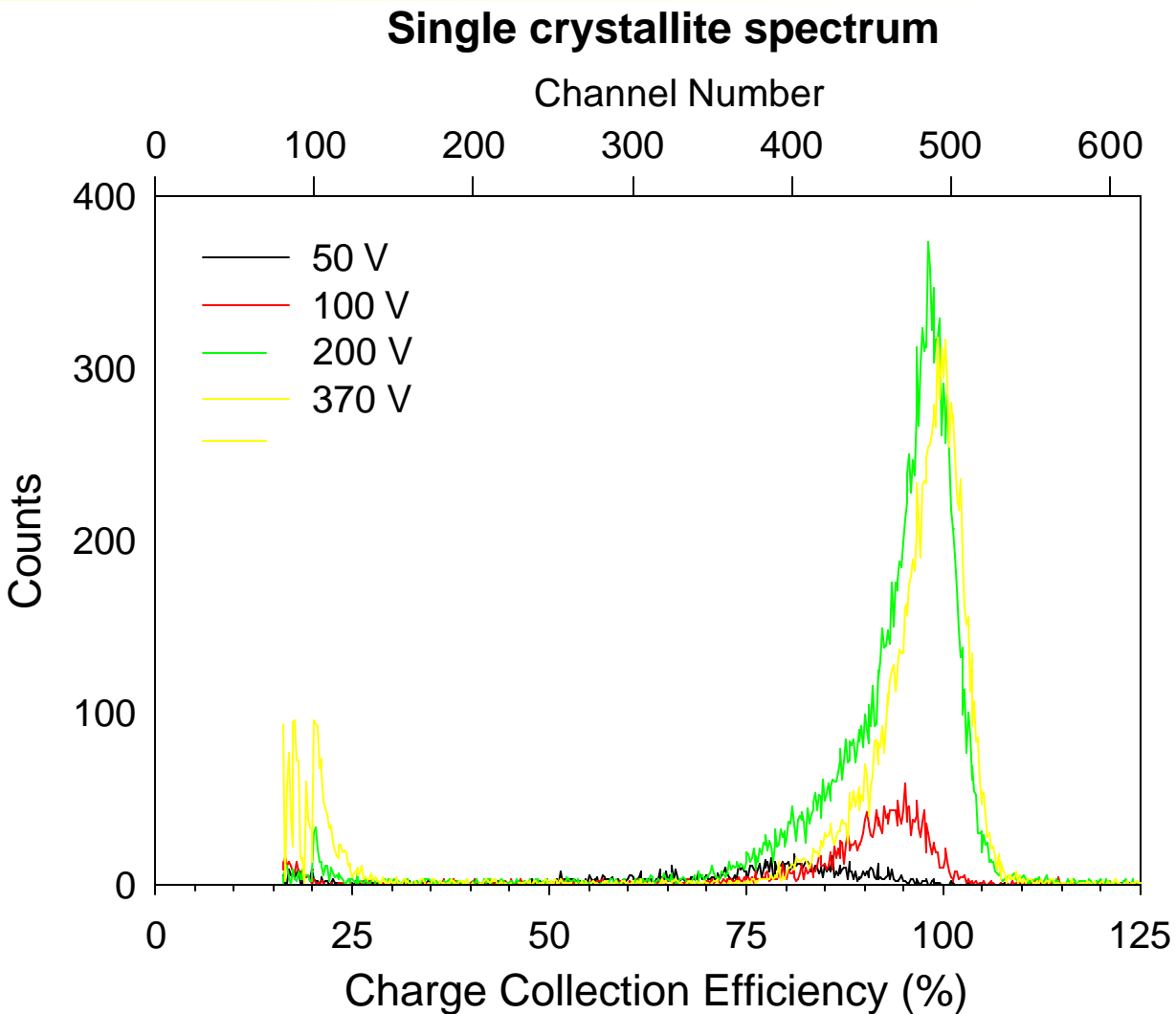
The IBIC data clearly follows the morphology of the grain and shows charge transport terminating at the grain edges.

Intra-crystallite charge collection efficiency



IBIC system records a full pulse height spectrum at each pixel in the image

Pulse height spectra vs. bias voltage

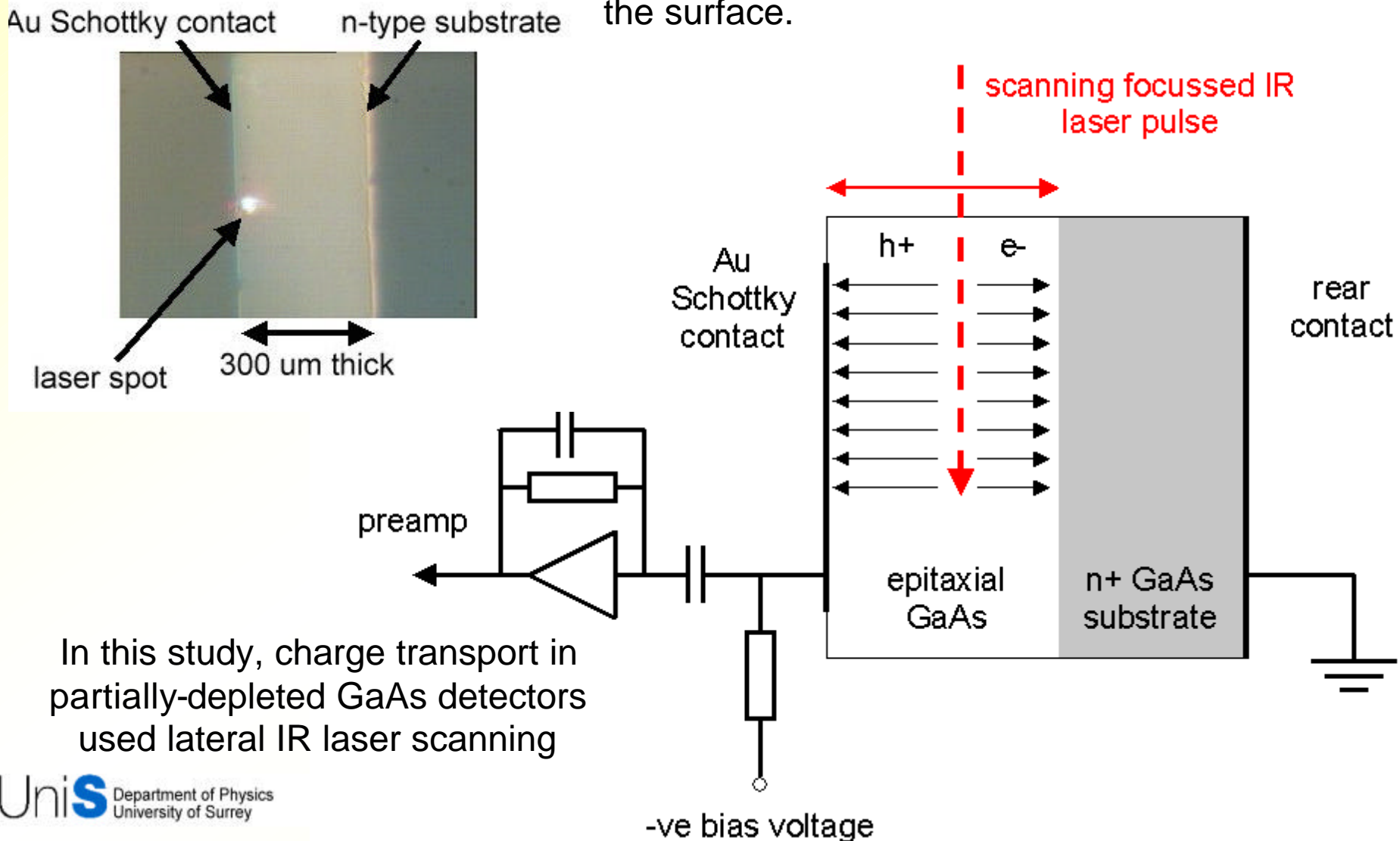


100% CCE is observed within a single large crystallite that lies between two electrodes

We see no evidence for gain mechanisms giving >100% CCE

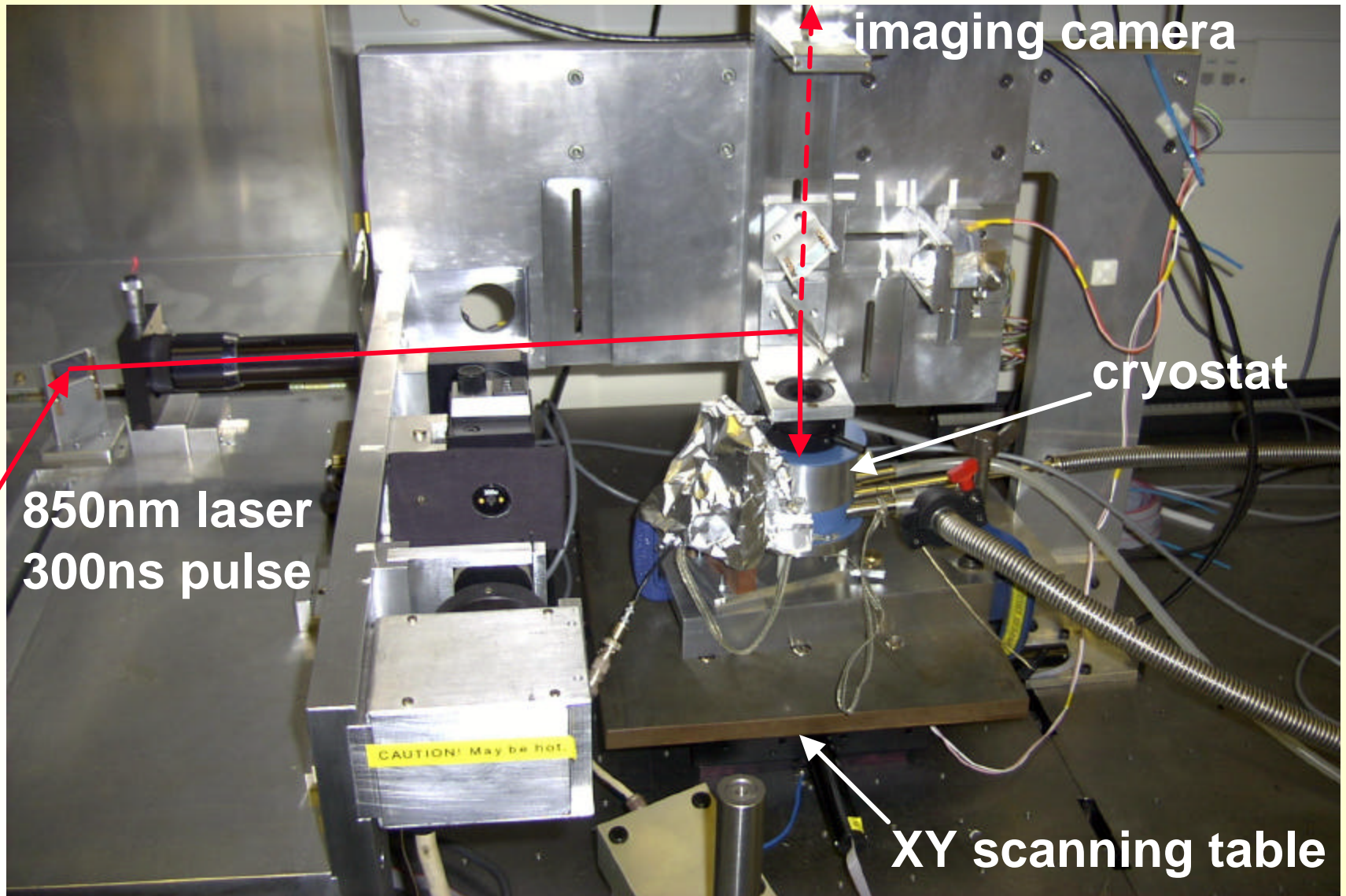
Focussed IR laser scans

For 50 - 100 μm spatial resolution, laser scanning provides a convenient mechanism to map CCE and E-field profiles. Sub-bandgap IR probes the bulk, red lasers tend to probe the surface.



In this study, charge transport in partially-depleted GaAs detectors used lateral IR laser scanning

Scanning optical bench



Laser pulse shapes

$T=273\text{K}$, 20V

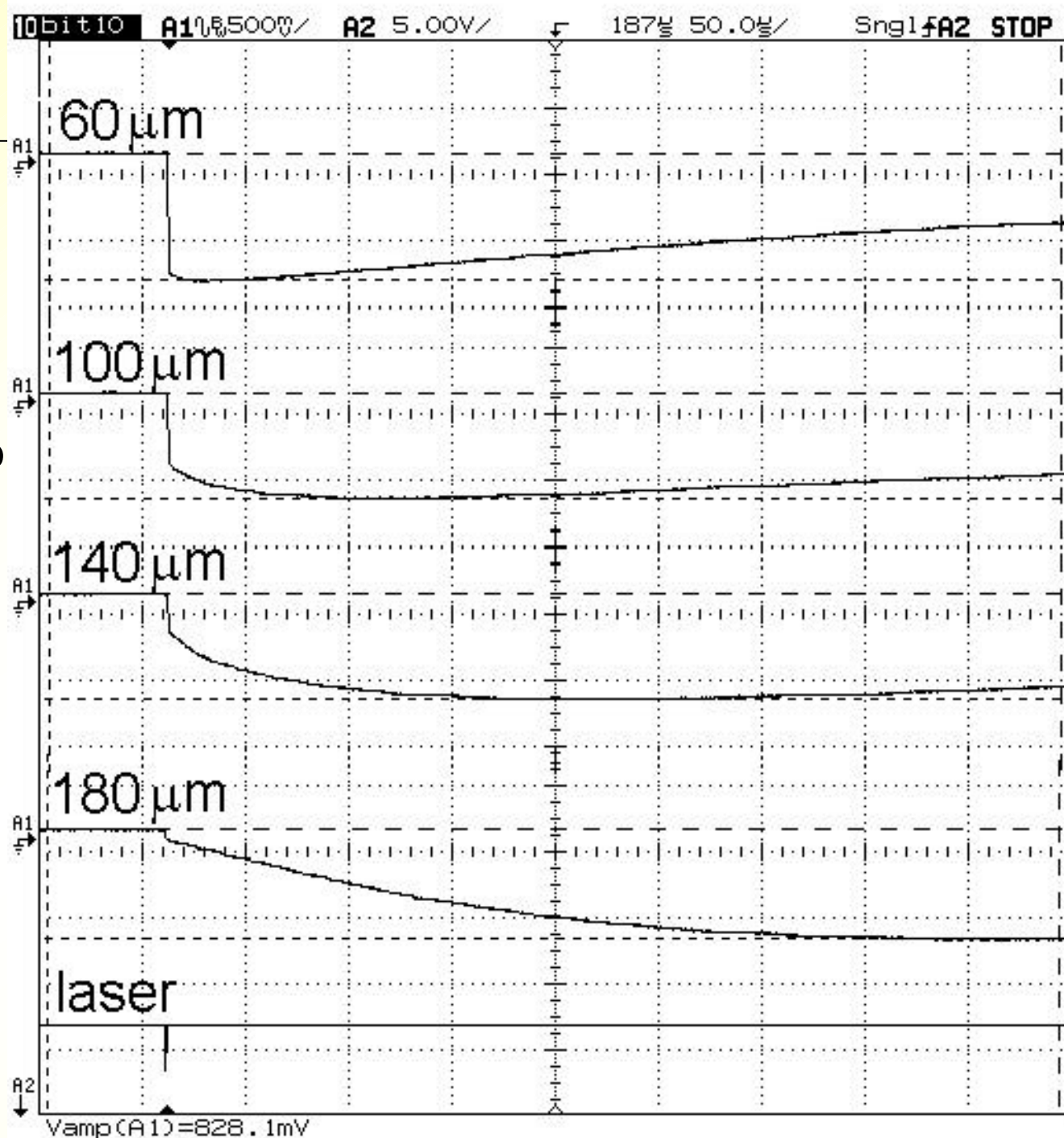
At $60\mu\text{m}$ from cathode:

no slow component to signal

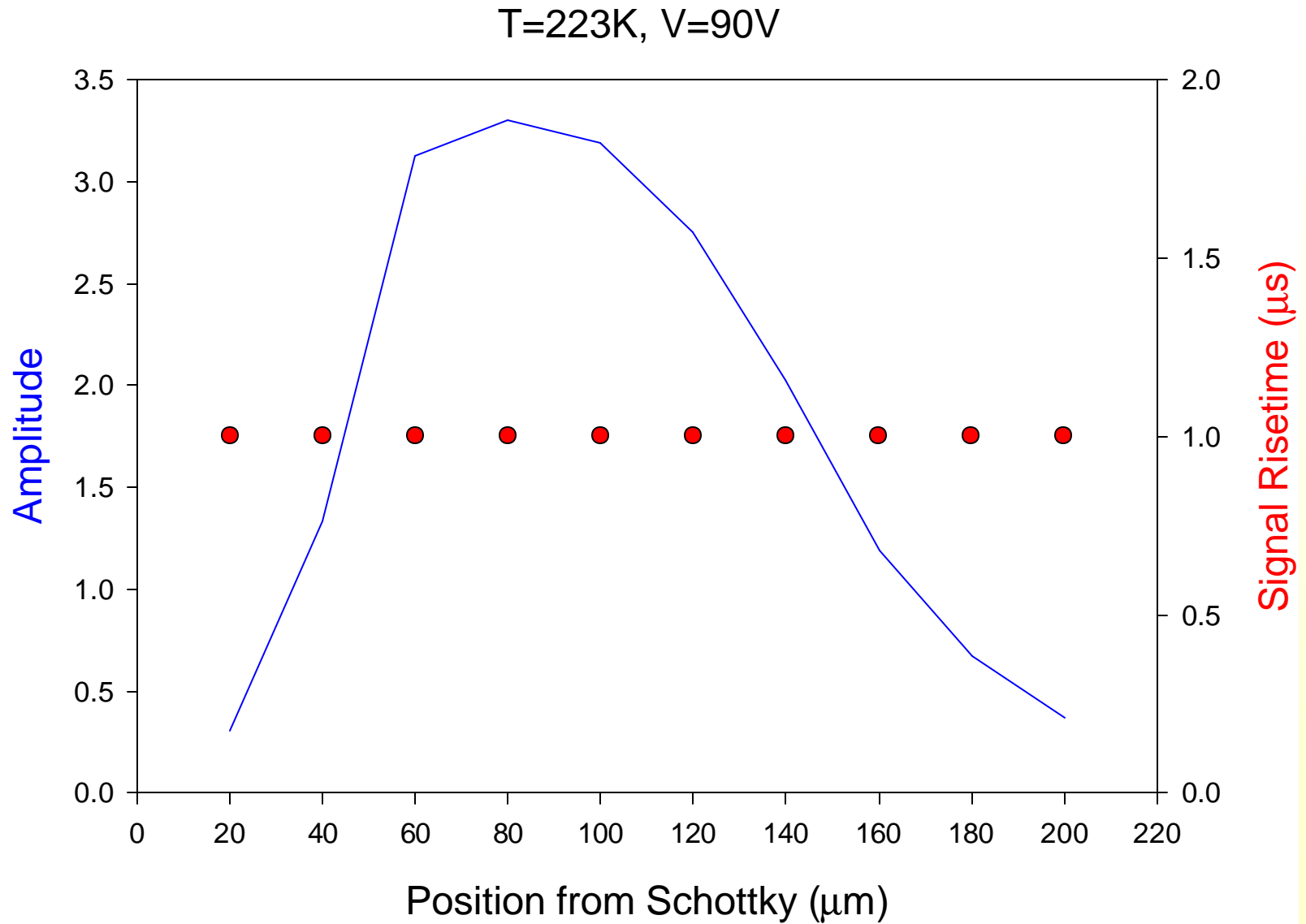
At $180\mu\text{m}$ from cathode:

charge drift times are $\sim 350\mu\text{s}$

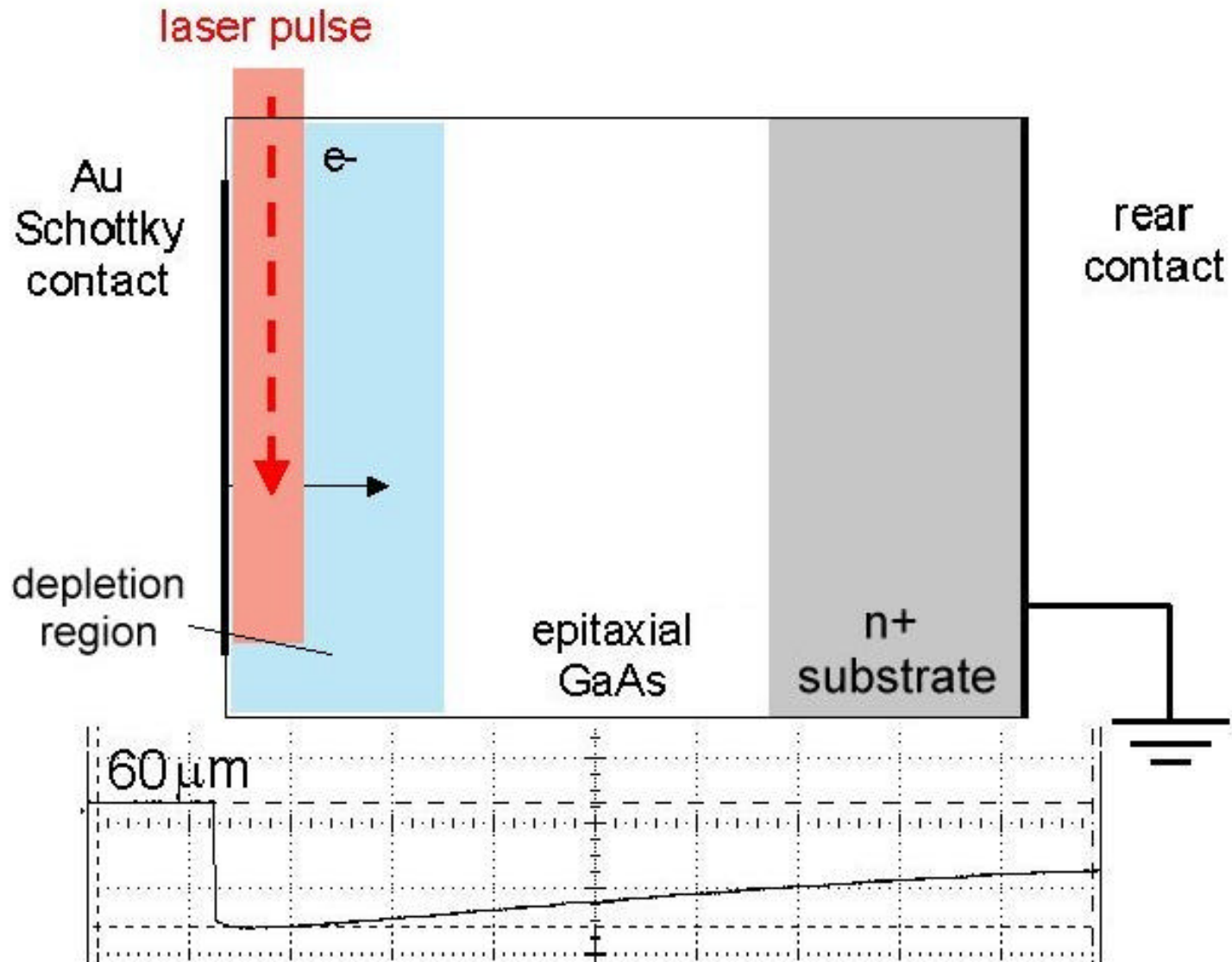
IR laser spot appears to have significant beam waist



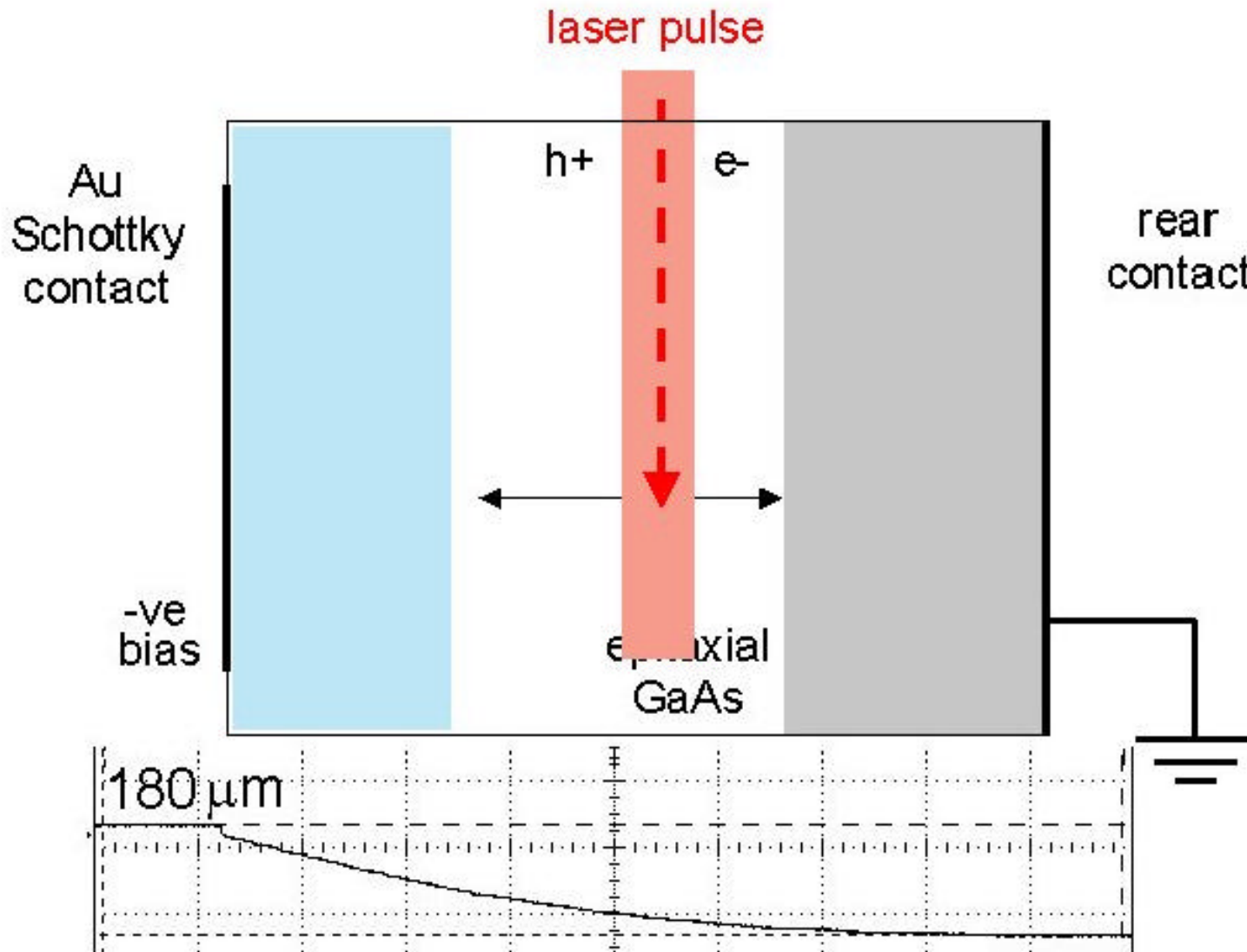
Pulse risetime and amplitude vs bias



Interaction close to the anode - inside depletion region



Interaction close to n+ substrate - in low field region



Conclusions

A range of optical, electrical and radiation techniques can be used to characterise new materials, specifically:

- material uniformity
- mu-tau products and CCE
- radiation hardness and characterisation of radiation-induced traps
- robust contact technologies

In the framework of RD50 materials such as SiC, a-Si and GaN are of particular interest.

Supply of high quality semi-insulating material from commercial vendors needs to be developed (eg, SiC from Cree, GaN from Kymatech).

Fabrication of standard test structures and protocols for characterisation will allow direct comparison between institutes.

Collaboration with the 'material characterisation' sub-group will be vital.



Facilities in the Group

Semiconductor detector laboratories:

- Optical and electrical characterisation (PICTS, DLTS, PL, Raman)
- Detector mapping systems using microfocus lasers and collimated radioisotopes

Ion Beam accelerator lab:

- new 6 MeV proton, 3 MeV alpha particle accelerator
- sub micron resolution nuclear microprobe for detector imaging
- implantation and damage studies

Device Fabrication: semiconductor clean room, photolithography

Device simulation: 3D device modelling (Silvaco), MCNP, EGS4, Geant

X-ray laboratory: X-ray sources 50-200 keV, Philips Fluorex monoenergetic X-ray source, image intensifiers, X-ray μ -CT

Radiation Physics: >130 sources including:

- Am:Be neutron sources (up to 18 GBq)
- ^{60}Co 'hot spot' irradiator (1.9 TBq), ~2.5 kGy per day

Polycrystalline Mercuric Iodide HgI_2

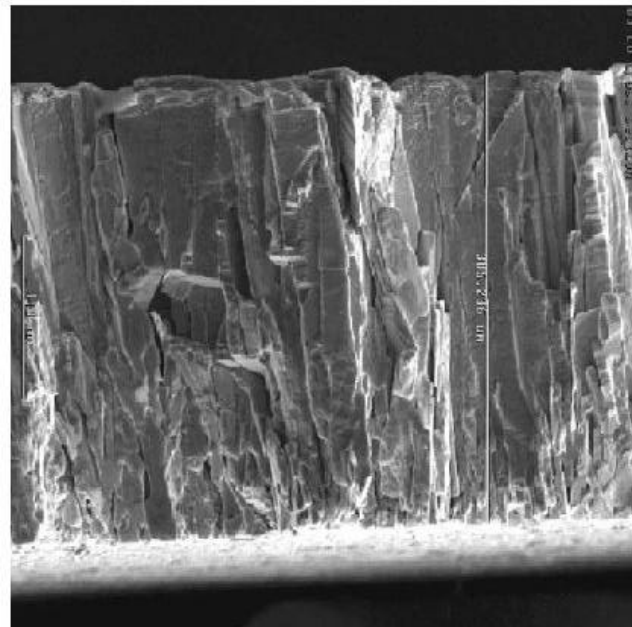
Single crystal HgI_2 is attractive for gamma ray imaging due to high atomic number (80, 53) with $\rho \sim 10^{13} \Omega\text{cm}$

Electron $\mu\tau \sim 10^{-4} \text{ cm}^2/\text{V}$, but hole $\mu\tau$ is $\sim 10^{-6} \text{ cm}^2/\text{V}$

Polycrystalline HgI_2 offers a low cost large area detector material, fabricated by screen printing of ceramic:

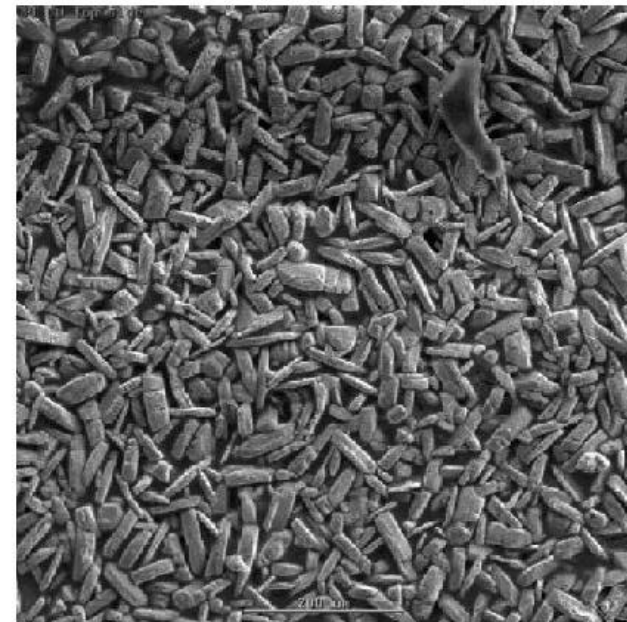
□ electron $\mu\tau \sim 10^{-7} \text{ cm}^2/\text{V}$

(cf. diamond $\mu\tau \sim 10^{-6} \text{ cm}^2/\text{V}$, selenium $\mu\tau \sim 10^{-5} \text{ cm}^2/\text{V}$)



Evaporated material gives better charge transport, and shows columnar growth similar to CVD diamond

M. Schieber et al, J. Cryst. Growth
225 (2001) 118-123



Other single crystal materials

Other bulk materials show promise for single element radiation detectors, but are not yet ready for commercial use:

Gallium Nitride

Single crystals of GaN have been developed in Warsaw

Grown in liquid Ga with N_2 over pressure: 20 kbar and 1700 °C

Undoped

⇒ n-type at 10^{19} cm^{-3} , $\rho \sim 10^{-3}\text{-}10^{-2} \Omega\text{cm}$

Grown with 0.5% Mg

⇒ semi insulating, $\rho \sim 10^4\text{-}10^6 \Omega\text{cm}$

SI material has residual concentration of $\sim 10^{16} \text{ cm}^{-3}$ - very poor charge transport

S. Porowski, *J Cryst Growth* 189/190 (1998) 153-158

GaN single crystal
(1mm grid)

